

# SEMI-CONTINUOUS ANAEROBIC CO-DIGESTION OF CHICKEN MANURE AND STRAW: PROCESS CHARACTERISATION AND MICROBIAL COMMUNITY DYNAMICS

## 鸡粪与秸秆半连续厌氧共消化特性研究及微生物群落变化分析

Chundong WU<sup>1</sup>), Chenxi LI<sup>1</sup>), Mingya WANG<sup>1</sup>), Zhanbin GUO<sup>\*1</sup>)

<sup>1</sup>)College of Engineering, Heilongjiang Bayi Agricultural University, Daqing/P.R.China

Tel: +86-459-13836962678; E-mail: 329984136@qq.com

Corresponding author: Zhanbin Guo

DOI: <https://doi.org/10.35633/inmateh-78-56>

**Keywords:** anaerobic co-digestion, semi-continuous, organic load rate, chicken manure

### ABSTRACT

Aiming to address the scarcity of semi-continuous experimental studies on chicken manure (CM) and corn stover (CS), as well as the unclear patterns of microbial community changes during digestion, this research employs both sequential batch and semi-continuous experimental methods for investigation. Sequential batch experiments showed that the anaerobic co-digestion (ACoD) of CM and CS had the highest cumulative methane yield ( $82.45(\pm 0.80)$  mL/g VS), high  $R_m$  and small  $\lambda$ , while the ammonia nitrogen ( $\text{NH}_4\text{-N}$ ) concentration generated during the reaction process was below the threshold of inhibitory concentration, indicating that CM and CS were more suitable as an anaerobic digestion (AD) substrate. The semi-continuous experiments showed that the maximum total daily gas production rate of 649.15 mL/gVS was achieved at an organic load rate (OLR) of 0.31 gVS/(L·d).  $\text{NH}_4\text{-N}$  concentration up to 4214.5 mg/L inhibited the semi-continuous flow digestion system. Microbial analysis showed that Firmicutes, Bacteroidota, and Proteobacteria were the dominant phyla throughout the AD experiment. *Sedimentibacter*, *Breznakibacter*, *Methanosarcina*, and *Methanobacterium* were significantly and positively correlated with methane production and improved the performance of CM treatment with CS. This study analysed the semi-continuous AD of CM and CS under different OLR, which can provide a reference for engineering applications.

### 摘要

为解决鸡粪与玉米秸秆连续实验研究匮乏及消化过程中微生物群落变化规律不明晰的问题，本研究采用序批式与半连续实验方法进行联合探究。序批式实验表明，鸡粪和玉米秸秆共消化具有最高的累计甲烷产率( $82.45(\pm 0.80)$  mL/g VS)、较高的甲烷生产速率和较小的滞后期。同时反应过程产生的氨氮浓度处于抑制浓度阈值以下，表明鸡粪和玉米秸秆更适合作为厌氧消化底物。半连续实验表明，当有机负荷率为0.31g VS/(L·d)时，日总产气量最高，达到649.15 mL/gVS。氨氮浓度高达4214.5 mg/L时，半连续流消化系统受到抑制。微生物分析表明，在整个实验过程中，Firmicutes、Bacteroidota、Proteobacteria是优势菌门。*Sedimentibacter*、*Breznakibacter*、*Methanosarcina*和*Methanobacterium*与甲烷产量呈显著正相关关系，并提高了鸡粪和玉米秸秆的处理效率。本研究分析了不同有机负荷率下鸡粪和玉米秸秆的半连续厌氧消化过程，为工程应用提供了参考依据。

### INTRODUCTION

Agricultural wastes such as animal manure need to be reasonably disposed of and utilised in a resourceful manner (Koul et al., 2022). China produces about 3.8 billion tons of animal manure annually, and the comprehensive utilisation efficiency is less than 60%. Untreated animal manure poses a serious threat to the environment, and direct irrigation of farmland can cause soil compaction, and the accumulation of harmful substances in the soil can affect crop growth (He et al., 2025). Therefore, it is important to dispose of animal manure reasonably. AD is the process of using anaerobic microorganisms to degrade organic matter (OM) in biomass and produce a mixture of gases, mainly  $\text{CH}_4$  and  $\text{CO}_2$ . Its advantage lies in the generation of energy gas, low energy consumption, and the production of digestate that can be used as fertiliser for field application, thereby achieving the reduction, harmlessness and resource utilisation of most organic wastes (Zhu et al., 2022; Zheng et al., 2022).

<sup>1</sup>Chundong Wu, Ph.D.; Chenxi Li, Prof. Ph.D.; Mingya Wang, MS; Zhanbin Guo, Prof. Ph.D.;

China produces approximately 155 million tons of CM annually. Due to its high total solids and volatile solids content, coupled with high biodegradability, CM is considered an ideal substrate for AD, possessing significant potential for bioenergy production. However, unlike other animal manures, CM exhibits a low carbon-to-nitrogen ratio (C/N) (approximately 8-10). This low C/N ratio leads to  $\text{NH}_4^+\text{-N}$  accumulation during AD.  $\text{NH}_4^+\text{-N}$  and organic acids are recognised as the most significant inhibitors of AD (Zhan *et al.*, 2026). The generally accepted optimal C/N ratio typically ranges between 20 and 35. In contrast, CS exhibits a high C/N ratio of approximately 60. This is attributed to the substantial organic carbon compounds produced through photosynthesis, coupled with corn's inherently low nitrogen use efficiency. Numerous studies have demonstrated that ACoD of CM with straw achieves nutritional optimization through substrate complementation: their synergistic effects regulate the system C/N ratio to the optimal range for AD (20-30), thereby alleviating the dual constraints of  $\text{NH}_4^+\text{-N}$  inhibition and carbon deficiency. Meanwhile, CM provides abundant nitrogen and trace elements, while straw supplies the carbon backbone necessary for volatile fatty acid synthesis, collectively facilitating methanogenic metabolism (Khatun *et al.*, 2025; Zhu *et al.*, 2022; Guo *et al.*, 2022).

The core research approach involves overcoming the limitations of single substrates through co-digestion for nutritional balance, pretreatment to enhance straw accessibility, and optimization of reactor operational parameters. However, existing studies still present the following deficiencies: current research predominantly focuses on batch AD, while semi-continuous operation—a mode more representative of engineering practice—remains insufficiently investigated regarding process stability, OLR regulation strategies, and long-term operational characteristics. Under semi-continuous conditions, the inhibition threshold of  $\text{NH}_4^+\text{-N}$ , the succession patterns of microbial communities, and their mechanistic associations with process performance lack systematic elucidation. Furthermore, research on the identification of key functional microorganisms and their abundance optimization in CM and CS ACoD systems warrants deeper investigation. Therefore, clarifying the synergistic response mechanisms among process parameters, microbial communities, and biogas production performance under semi-continuous operation, and establishing process optimization strategies based on microbial regulation, constitute the critical scientific issues for achieving efficient and stable ACoD of CM and CS.

To address these research gaps, this study proposes to systematically investigate the interaction mechanisms during the ACoD of CM and CS through a combined approach of batch and semi-continuous experiments. The research will focus on analysing process stability,  $\text{NH}_4^+\text{-N}$  inhibition thresholds, and microbial community succession patterns under various OLR, identifying key functional microorganisms and elucidating their ecological functions. The ultimate goal is to provide theoretical foundations and technical references for the artificial regulation of long-term stable operation of mesophilic semi-continuous flow AD processes for CM.

## MATERIALS AND METHODS

### *Substrate properties and inoculum characteristics*

The DM, SM, and CS used in the experiment were obtained from a farmer in Lindian County, Daqing City, Heilongjiang Province, and the CM was obtained from a large chicken farm in Daqing City, Heilongjiang Province. The three manure samples were first cleared of debris, then stirred separately until homogeneous, and stored in a 4°C refrigerator for later use. The CS was cut and crushed into fine stover granules, which were sieved through a 40-mesh sieve. Based on the previous research of the group, frozen pretreatment was applied to the CS. The inoculum was the digested liquid in the continuous flow reactor of long-term stable operation in the laboratory, which was incubated at a medium temperature (37°C±0.5°C) until it was no longer produced gas was produced and then prepared for use. The substrate and inoculum characteristics are shown in Table 1.

**Table 1**

Substrate and inoculum properties			
Raw material	Total solid (TS) [%]	Volatile solid (VS) [%]	VS/TS [%]
DM	20.53±1.49	16.06±0.76	78.30±1.96
SM	27.32±0.64	20.86±1.72	75.03±7.12
CM	30.97±0.77	18.17±1.18	51.01±1.29
CS	93.23±0.28	78.86±1.15	84.59±0.98
Inoculum	6.82±0.14	4.51±0.09	66.16±0.08

### Configuration and operation of sequential batch and semi-continuous reactors

Pre-sequence batch experiments were carried out in a small anaerobic reaction setup (Fig. 1(a)). The experimental setup, model blue-cap reagent bottle, was obtained from Sichuan Shubo Group Co., Ltd. (Sichuan, China). The experimental setup had a volume of 250 mL, and both outlets were connected to latex rubber tubing and sealed with a pinch clamp. A 0.5 L gas collection bag was connected to the latex tube for collecting biogas, and another latex tube was connected to a manometer for measuring the biogas production. The temperature control equipment was a light-controlled shaking incubator (Shanghai Shiping Experimental Equipment Co., Ltd., JDX-211C-GZ), which controlled the digestion temperature at  $37 (\pm 0.5) ^\circ\text{C}$ . Later, a continuous stirred tank reactor (CSTR) (Beijing Bichen Instrument Co., SIGTUNA KR3T-5) was used for the semi-continuous AD experiment of CM and CS, as shown in Fig. 1(b). The total volume was 5 L, and the effective volume was 3.5 L. The CSTR tank was of double-wall structure with a water bath jacket on the outer wall, which could control the temperature of the reactor to  $37 (\pm 0.5) ^\circ\text{C}$  throughout the experiment. The top of the digestion tank is equipped with two calibre feed ports, and the bottom of the digestion tank is the discharge port. The top of the tank is a mechanical sealing device with good tightness, and there is a stainless-steel stirring paddle, and the stirring speed is controlled by a governor at 60 r/min.



**Fig. 1 - Anaerobic digestion setup**

(a) Sequential batch experimental setup

(b) Semi-continuous flow experimental setup

### Experimental protocols for sequential batch and semi-continuous AD

1) A sequential batch experiment was used to study the gas production characteristics of the AD of different animal manures. To ensure comparability among different manure types, the VS concentrations of DM, SM, CM, and CS were uniformly standardized to 5%. This normalization approach was adopted to eliminate the confounding effects of OLR, thereby enabling direct comparison of the intrinsic digestion characteristics of different substrates. The selection of 5% VS concentration was based on the following considerations: this concentration represents a medium solids level within the typical range for mesophilic AD of livestock manures (4-10% VS); it effectively avoids ammonia inhibition, which is particularly critical for nitrogen-rich CM; and it prevents rapid acidification commonly observed in SM under high-loading conditions. The experiment was set up with a manure single-digestion treatment group and a CS co-digestion treatment group, with three kinds of manure. Based on preliminary results from our laboratory and previous reports in the literature, the three types of manure were individually mixed with CS at a VS mass ratio of 1:1 (He *et al.*, 2025). Based on the preliminary experimental results, all treatments exhibited superior cumulative methane yield and system stability at an inoculum-to-substrate ratio of 1:1 (based on VS). Therefore, this inoculum-to-substrate ratio was adopted for the formal experiments in this study. A total of 6 treatments were established, with 3 parallel replicates per treatment. The amount of substrate filled in each reactor is shown in Table 2. The materials were sealed immediately after bottling, and then each treatment was placed in a light-controlled shaking incubator with the digestion temperature controlled at  $37 (\pm 0.5) ^\circ\text{C}$ .

2) A semi-continuous experimental method was used to study the effect of different OLR on the AD process of CM and CS. CM and CS were mixed according to the VS mass ratio of 1:1 (He *et al.*, 2025). The VS mass fraction of the mixed substrate was maintained at a relatively low level of 6% to ensure slurry homogeneity and facilitate feeding and discharge operations (Gong, S.Y., 2020). The inoculum ratio (based on the VS content) was 1. Before conducting the experiment, 2,380 mL of inoculum, 288 g of CM, and 66 g of CS were added to the reactor, and then deionised water was added to bring the total mass of the feedstock to 3.5 kg and stirred to mix. The reactor temperature was set at mesophilic conditions of  $37 (\pm 0.5) ^\circ\text{C}$ .

Based on previous studies, the hydraulic retention time (HRT) was 20 days, and the experimental period was 100 days. Stirring was done every 12 h for 30 min at a speed of 60 r/min, and the gas production was recorded once a day at regular intervals. Main physicochemical parameters of the daily digested effluent were determined. The reactor was set up with one experimental group and three parallel replicates. Daily feed amounts for different OLR are shown in Table 3.

Table 2

Substrate loading schedule for sequencing batch experiments

Substrate	Amount of substrate added [g]	Amount of inoculum added [g]	Total amount [g]
DM	31.13	110.86	141.99
SM	23.97	110.86	134.83
CM	27.52	110.86	138.38
DM+CS	15.57+3.17	110.86	129.6
SM+CS	11.98+3.17	110.86	126.01
CM+CS	13.76+3.17	110.86	127.79

Table 3

Feeding schedule for semi-continuous experiment

HRT [d]	Feed quantity [L/d]	Feed [%]	OLR [gVS/(L·d)]	CM [g]	CS [g]	Water [g]
0~20	0.175	6.12	0.31	29.47	6.79	138.74
21~40	0.381	7.65	0.82	80.21	18.48	282.31
41~60	0.587	9.69	1.63	156.52	36.06	394.42
61~80	0.278	6.63	0.53	50.72	11.68	215.59
81~100	0.484	8.67	1.20	115.47	26.61	341.92

### Indicators and methods of analysis

1) Gas production analysis. Daily biogas production was calculated using a manometer (Zhibiao Instrument Co., Ltd., GM522) measurement, and methane concentration was determined using a gas chromatograph (Shimadzu Corporation, GC-2014-C). A modified Gompertz model was used to fit the experimental cumulative methane production rate to predict the performance parameters of AD, as shown in equation (1).

$$G(t) = G_{max} \exp\{-\exp [R_m e / G_{max} (\lambda - t) + 1]\} \quad (1)$$

where  $G(t)$  is the specific methane production at a given time  $t$ , mL/g VS;  $G_{max}$  is the maximum methane potential of the feedstock, mL/g VS;  $R_m$  is the maximum methane production rate, mL/g VS·d;  $\lambda$  is the lag period, d;  $t$  is the digestion time, d; and  $e = 2.7183$ .

2) Physical and chemical index analysis. TS and VS were determined using the cauterisation method (GB/T28731-2012), and pH was determined using a pH meter (Shanghai Leici Marketing Centre, PHSJ-4F). SCOD,  $\text{NH}_4\text{-N}$ , total nitrogen (TN), and total phosphorus (TP) were determined using a UV-visible Intelligent Multi-Parameter Water Quality Analyser (Beijing Lianhua Yongxing Technology Development Co., Ltd., LH-3BA (V10)).

3) Nutrient index analysis. OM, hydrolysable nitrogen (HN), and available Potassium (AK) were determined according to the standards NY/T 1121.6-2006, LY/T 1228-2015, and NY/T 889-2004, respectively, and available phosphorus (AP) was determined by sodium bicarbonate extraction - molybdenum-antimony anti-spectrophotometric method (HJ 704-2014).

4) Microbial community analysis. The microbial community analysis of the digested samples was determined by a high-throughput sequencing method by Shanghai Personal Biotechnology Co., Ltd.

### Data analysis

Experimental data were expressed as mean  $\pm$  standard deviation. Spearman correlation analysis was performed between microbial community and methane production, with significance testing. Data processing was conducted using Microsoft Excel 2017, and data fitting and graphing were performed using OriginPro 2017.

## RESULTS AND DISCUSSIONS

### Results of sequential batch experiments

#### Cumulative methane yield and kinetic parameters of AD

Methane yield is the main indicator of the performance of the AD of organic waste. Fig. 2 shows the cumulative methane yield of the AD experiment for each treatment and the Gompertz fitted curve for each treatment. Table 4 shows the performance parameters of AD for each treatment predicted by the modified Gompertz model, including  $G_{max}$  (mL/g VS),  $R_m$  (mL/g VS·d), and  $\lambda$  (d).

As shown in Fig. 2(a), the cumulative methane yields of CM, SM and DM were 80.64 ( $\pm 0.41$ ) mL/g VS, 46.42 ( $\pm 0.72$ ) mL/g VS and 6.42 ( $\pm 0.76$ ) mL/g VS, respectively, and the highest cumulative methane yields were found in CM, which were 1.74 and 12.56 times higher than those of SM and DM, respectively. This is consistent with the research findings reported by Sun et al., which state that "the content of easily degradable components in faecal substrates from high to low is CM (59.73%), SM (47.08%), and DM (39.49%)," indicating that CM has superior methane production potential due to its higher content of easily degradable components (Sun et al., 2025). However, the high nitrogen content in CM may result in excessive ammonia release, consequently inhibiting the AD process. Table 4 presents the AD performance parameters fitted by the Gompertz model. As shown in Table 4, the adjusted  $R^2$  values are all greater than 0.96, indicating that the Gompertz model provides a good fit for all treatment groups. CM exhibited the highest  $G_{max}$  and  $R_m$  values, both of which were higher than those of SM and DM, indicating that CM possesses the greatest biogas production potential and the fastest biogas production rate. Meanwhile, CM exhibited the lowest  $\lambda$  value, indicating the shortest lag phase and start-up time, suggesting the most rapid microbial acclimation and methanogenesis. The gas production performance of CM was superior to that of DM and SM, mainly in terms of higher cumulative methane production, higher  $R_m$ , and shorter  $\lambda$ . Analysed in terms of the content of readily degradable components, CM usually contains high levels of readily degradable OM (e.g., proteins, fats, uric acid, etc.), which is an important reason why it is a good methane substrate. Analysed in terms of C/N, CM usually has a low C/N. A low C/N implies a high ammonia level, which inhibits microbial activity (especially methanogens); however, under certain optimised conditions (e.g., co-digestion, dilution, etc.), CM's own rich organic substrate can still provide a higher methane potential (Song et al., 2023).

Another study showed that ACoD of animal manure with crop residues could improve the gas production efficiency. Fig. 2(b) shows the variation of the cumulative methane production rate of ACoD of three types of manure with CS in the same ratio. From Fig. 2(b), it can be seen that the cumulative methane yield of manure-straw co-digestion had the same trend as that of manure mono-digestion. The highest cumulative methane yield was found in CM + CS co-digestion (82.45 ( $\pm 0.80$ ) mL/g VS), which was 2.2% higher compared to CM mono-digestion (80.64 ( $\pm 0.41$ ) mL/g VS). The cumulative methane yield of DM + CS (16.81 ( $\pm 0.63$ ) mL/g VS) was 61.8% higher than that of DM mono-digestion (6.42 ( $\pm 0.76$ ) mL/g VS). The cumulative methane yield of SM + CS (52.43 ( $\pm 0.53$ ) mL/g VS) increased by 11.5% compared to SM mono-digestion (46.42 ( $\pm 0.72$ ) mL/g VS). As shown in Table 4, CM+CS treatment had higher  $G_{max}$ ,  $R_m$ , and lower  $\lambda$  values, showing better AD performance. Although CM co-digested with CS exhibited the optimal AD performance, its synergistic enhancement effect with CS was weaker than that of SM and DM systems. This phenomenon may imply limitations in nutritional complementarity and microbial metabolic synergy between CM and CS.

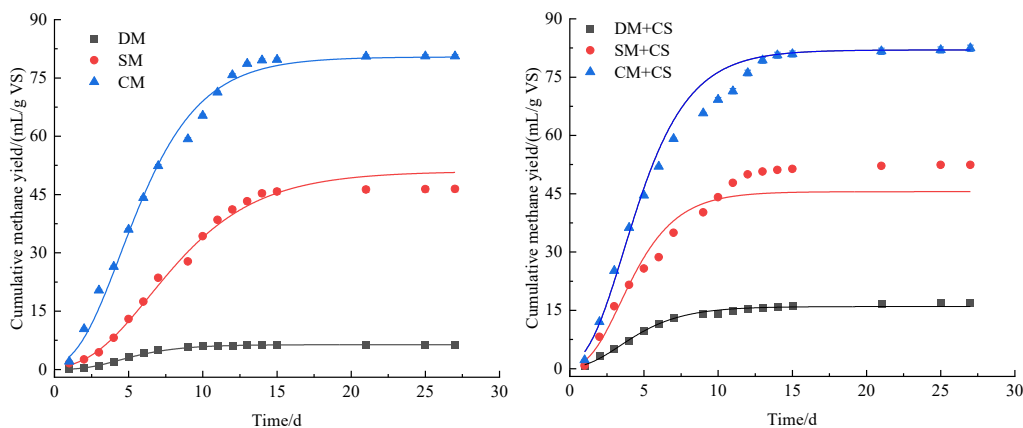


**Fig. 2 - Cumulative methane yield with modified Gompertz fit curve**

(a) Manure mono-digestion

(b) Co-digestion of manure and straw

Table 4

Performance parameters of the Gompertz model fit				
Substrate	$G_{max}$ [mL/g VS]	$R_m$ [mL/g VS-d]	$\lambda$ [d]	Adjusted R-squared
DM	6.37±0.027	1.03±0.034	2.04±0.063	0.999
SM	50.98±3.374	4.69±0.195	2.37±0.117	0.985
CM	80.41±1.635	10.046±0.452	1.49±0.134	0.995
DM+CS	15.98±0.300	2.52±0.098	1.04±0.094	0.994
SM+CS	45.54±2.898	7.98±0.716	1.28±0.132	0.968
CM+CS	82.02±2.125	12.44±0.655	1.189±0.061	0.981

### Concentration of SCOD and $NH_4^+-N$ in the digestate effluent

The change of SCOD in the digestate effluent can characterise the hydrolysis efficiency of the substrate in the presence of anaerobic bacteria. Samples of each group of digestate effluent were taken and measured at intervals of 7 days in the experiment, and the changes in SCOD concentration in each group of digestate effluent are shown in Fig. 3(a). The highest SCOD concentration was found in CM, indicating that the effective OM available for methanization was more abundant, which is mainly attributed to the higher protein and nitrogenous OM content in CM. At the beginning of the experiment, the SCOD of the CM group had a slow increasing trend, and was in a decreasing trend from the 7th day until the late stage. While the SCOD of DM and SM groups had roughly the same pattern of change, decreasing from 0-7 days, slowly increasing from 7-14 days, and then showing a decreasing trend. Under the same operating conditions, the SCOD levels of both CM and SM co-digestion systems were lower than those of the corresponding mono-digestion systems, indicating that the synergistic effect between the substrates in the co-digestion process facilitates the conversion of the soluble OM to the subsequent methanogenic stage and improves the efficiency of SCOD consumption. In contrast, the SCOD levels of the DM co-digestion system were higher than those of the corresponding mono-digestion system. This may be because single DM systems tend to have lower peak and total SCOD release due to nutrient imbalance and limited hydrolysis (Karki *et al.*, 2021). The SCOD concentration of each group decreased from 6471~11176 mg/L at the beginning of the experiment to 3662~6772 mg/L at the end of the experiment. The SCOD removal rates of DM, SM, CM, DM+CS, SM+CS, and CM+CS groups were 43.41%, 45.28%, 46.84%, 46.95%, 28.07%, 39.41%, respectively. The results showed that CM had the highest SCOD removal efficiency. Although mono-digestion of CM exhibited a higher SCOD removal rate, its cumulative methane yield was lower than that of the CM + CS co-digestion system. This phenomenon may be attributed to the low C/N ratio of CM, limiting the metabolic activity of methanogens.

The variation of an  $NH_4^+-N$  concentration in the digestate effluent is shown in Fig. 3(b). CM is a nitrogen-rich organic waste, and the  $NH_4^+-N$  concentration in the CM group was the highest at (2571.67±25.58) mg/L. Both DM and SM groups were relatively low at (622.2±12.52) mg/L and (883.47±4.41) mg/L, respectively. When CM, SM, and DM were co-digested with CS, the  $NH_4^+-N$  concentrations were (1637.14±5.13), (880.67±159.86), and (678.13±36.14) mg/L, respectively. Under the same operating conditions, the ammonia levels of the co-digestion system were lower than those of the corresponding mono-digestion system. Straw as a high-carbon co-substrate complemented the low C/N ratio of the animal manure, bringing the overall C/N ratio of the system closer to the optimal zone (about 20-30) for the AD flora. This helped to reduce the peak ammonia concentration from protein breakdown, thereby reducing net  $NH_4^+-N$  accumulation (Wang *et al.*, 2024). An appropriate  $NH_4^+-N$  concentration can increase the buffering capacity and stability of the AD system. Excessive  $NH_4^+-N$  concentration can hinder the metabolism of acetate, causing inhibition of the reaction, and the inhibitory concentration is generally higher than 3000 mg/L. Therefore, the  $NH_4^+-N$  concentrations generated from CM and the co-digestion reaction process of CM and CS in this study were below the threshold of inhibitory concentration, which can provide a basis for the stable operation of the subsequent semi-continuous reaction.

The above analysis showed that the ACoD of CM and CS had the highest cumulative methane yield, high  $R_m$  and small  $\lambda$ , while the  $NH_4^+-N$  concentration generated during the reaction process was below the threshold of inhibitory concentration. Therefore, CM and CS were selected as substrates for ACoD in the subsequent continuous flow experiments.

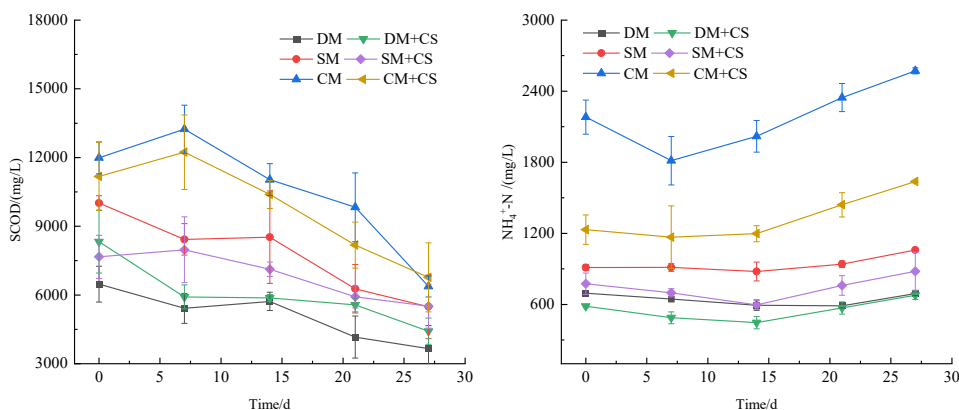


**Fig. 3 - SCOD concentration and NH<sub>4</sub><sup>+</sup>-N concentration in the digestate effluent**  
 (a) SCOD concentration (b) NH<sub>4</sub><sup>+</sup>-N concentration

**Results of semi-continuous flow experiments**

**Daily biogas production and daily methane yield**

The daily total gas production rate and daily methane production rate at different OLR are shown in Fig.4. When the OLR was 0.31 g VS/(L·d), the total daily gas production in this stage increased first and then decreased, with a maximum of 659.15 mL/g VS. When the OLR was increased to 0.82 g VS/(L·d), the total daily gas production rate decreased rapidly and was smoother in this stage, with a maximum of 143.58 mL/g VS. When the OLR continued to increase to 1.63 g VS/(L·d), the total daily gas production rate still showed a decreasing trend, with a maximum of 89.27 mL/g VS in this phase. Due to the increase in OLR, the reaction entered into a buffer period. At this time, the feeding and discharging were stopped to wait until the system was stabilised, and this phase lasted for 10 days. Subsequently, the OLR was reduced to 0.53 g VS/(L·d), and the total daily gas production rate was 84.91 mL/g VS in this phase, which was still in a decreasing trend. When the OLR was further increased to 1.20 g VS/(L·d), the biogas production performance continued to decline. It is possible that the high NH<sub>4</sub><sup>+</sup>-N concentration (as shown in Fig. 5) due to the excessive OLR in the previous period inhibited the activity of methanogenic bacteria, which prevented them from carrying out the methanogenic reaction properly, which in turn affected the biogas production (Duan et al., 2022). As can be seen from Fig. 4(b), the overall trend of the daily methane production rate and total daily gas production rate was the same throughout the reaction process.

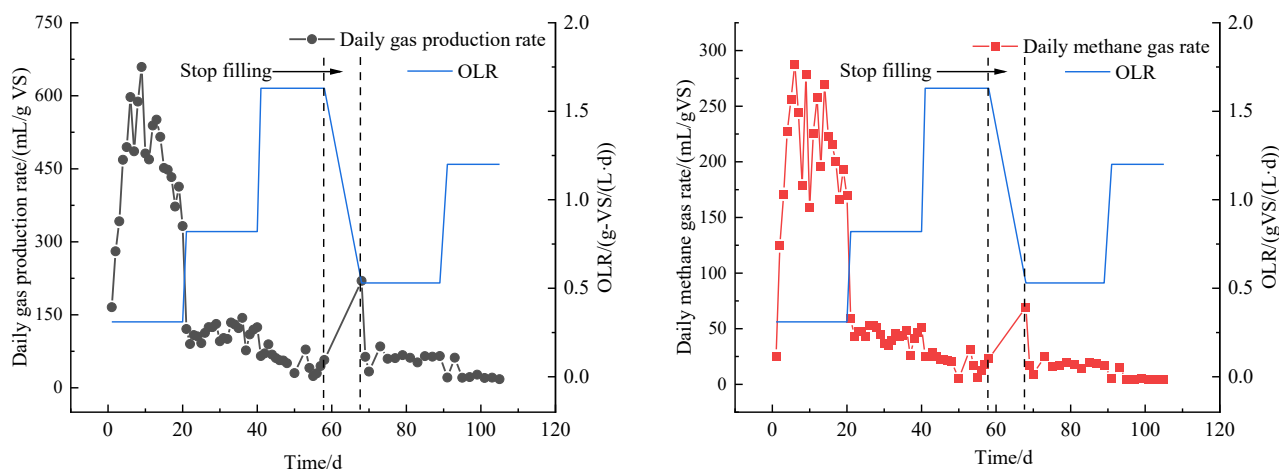


**Fig. 4 - Effect of OLR on gas production characteristics of CM**  
 (a) Change in total daily gas production rate (b) Change in daily methane production rate

At an OLR of 0.31 g VS/(L·d), the daily methane production rate showed a reciprocal trend, and the daily methane production rate peaked at 287.52 mL/g VS. Subsequently, the OLR began to increase, at which time the TS of the AD reaction continued to rise, and the reaction began to shift from wet AD to dry AD. When the OLR increased to 0.82 g VS/(L·d), the daily methane production rate, which was similar to the total gas production rate on the same day, decreased rapidly to 53.20 mL/g VS. When the OLR was 1.63 g VS/(L·d), the daily methane production rate was 31.53 mL/g VS, which further showed an even lower trend.

When the OLR was subsequently decreased to 0.53 g VS/(L·d) and increased to 1.20 g VS/(L·d), the daily methane production rate continued to decrease in both cases.

As can be seen from the comparison in Fig. 4, when the daily gas production rate decreased sharply, the daily methane production rate also decreased. As the OLR increased, the microorganisms needed to adapt to higher substrate concentrations and possible inhibitors (e.g.,  $\text{NH}_4^+\text{-N}$  and volatile fatty acids (VFAs)), and once the OLR exceeded the metabolic capacity of the microorganisms, it might lead to the accumulation of toxic substances and pH changes, which in turn led to the inhibition or imbalance of the digestive system. As a result, the digestive system had difficulty in restoring homeostasis, even when the OLR was adjusted to be lowered, and showed systemic overload due to the reaction stagnation on day 58.

Based on the above experimental results, the methane yield of the AD system reached its peak when the OLR was controlled at 0.31 g VS/(L·d).

### **Physical and chemical characterisation of digestate effluent**

Fig. 5 shows the trend of  $\text{NH}_4^+\text{-N}$ , TN, SCOD, and TP concentrations with time at different OLR.  $\text{NH}_4^+\text{-N}$  is a key indicator affecting the operational stability of the AD process. When the OLR was in the range of 0.31 g VS/(L·d) ~ 1.63 g VS/(L·d), the  $\text{NH}_4^+\text{-N}$  concentration in the digestate effluent gradually increased from 2170.5 mg/L to 4214.5 mg/L. This may be because high OLR promotes the rapid decomposition of proteins and nitrogenous substances, thus releasing more  $\text{NH}_4^+\text{-N}$ . When the OLR reached 1.63 g VS/(L·d), the total daily gas production rate at this OLR rapidly decreased to 89.27 mL/g VS, indicating that the high  $\text{NH}_4^+\text{-N}$  concentration of 4214.5 mg/L may have induced a significant inhibition of the semi-continuous flow AD of CM+CS. This is further supported by the rapidly decreasing gas production rate and daily methane production rate at this OLR, as shown in Fig. 4. When the OLR was reduced to 0.53 g VS/(L·d), the  $\text{NH}_4^+\text{-N}$  concentration began to decrease rapidly, further increasing the OLR to 1.20 g VS/(L·d) resulted in a stable  $\text{NH}_4^+\text{-N}$  concentration, but the gas production of the reaction was not improved. This may be due to the inhibition of methanogen activity. It has been noted that lower concentrations of  $\text{NH}_4^+\text{-N}$  can be used as an effective nitrogen source for microbial growth, and high concentrations of  $\text{NH}_4^+\text{-N}$  can inhibit the activity of methanogenic bacteria. For example, when the concentration of  $\text{NH}_4^+\text{-N}$  exceeds 3000 mg/L, ammonia is considered to be toxic and may produce ammonia inhibition and reduce methane production (Ngo *et al.*, 2024). The trends of TN and  $\text{NH}_4^+\text{-N}$  concentrations in the digestate effluent were approximately the same. This may be attributed to the fact that  $\text{NH}_4^+\text{-N}$  is the predominant form of nitrogen during AD, and its concentration variation governs the trend of TN.

At the beginning of the experiment, when the OLR was 0.31 g VS/(L·d), the SCOD concentration showed a smooth trend, and the concentration fluctuated around 12,000 mg/L. The total gas production increased and then decreased during this period, and the magnitude of the change was significant. This may be attributed to the acclimatization phase of microorganisms at the initial stage, where SCOD degradation was asynchronous with biogas production: the rapid release of readily degradable organics in the early phase led to increased gas production, followed by a decline due to substrate depletion in the later phase. When the OLR increased to 0.82 g VS/(L·d), the SCOD concentration increased significantly and peaked at day 37 (54,025 mg/L). At this time, there was a large accumulation of OM in the system, and the total gas production rate decreased sharply at this stage. This may be due to the high  $\text{NH}_4^+\text{-N}$  concentration, which has inhibited the digestion reaction. When the OLR increased by 1.63 g VS/(L·d), the SCOD concentration decreased significantly, and the gas production in this stage continued to decrease. The possible reason is that the high  $\text{NH}_4^+\text{-N}$  concentration leads to an imbalance in the AD process of the synergistic metabolism of a variety of microorganisms, which affects the stability of the AD system, and causes a significant decrease in the methane production in the reactor or even no longer produces gas (Mlinar *et al.*, 2022). After a 10-day feeding cessation, the OLR was further reduced to 0.53 g VS/(L·d), resulting in a significant increase in SCOD concentration. This was likely attributed to the rapid recovery of hydrolytic acidogenic bacteria, which caused the notable rise in SCOD, while methanogenic bacteria failed to recover synchronously due to prior ammonia inhibition (4214.5 mg/L), leading to carbon metabolism interruption at the acidification stage (Zhang *et al.*, 2022). Subsequently, increasing the OLR to 1.20 g VS/(L·d) promoted SCOD consumption but failed to alleviate biogas production, indicating that the methanogenic community had suffered irreversible damage and the system function was locked into the acidification process.

Phosphorus is one of the important nutrients for the growth of microorganisms, and the variation of its concentration may be related to the uptake and release of phosphorus by microorganisms as well as the chemical deposition of phosphorus.

When the OLR was 0.31 g VS/(L·d), the TP concentration was relatively smooth. With the continuous feeding and discharging during the reaction and the increase of OLR, the TP concentration increased from 16 mg/L to 92.35 mg/L with a continuous upward trend. After reducing the OLR, TP still showed an increasing trend (up to 108.25 mg/L). This may be due to the situation of phosphorus accumulation due to overloading or destabilisation of the AD system, which causes phosphorus to be deposited in an insoluble form (Xu *et al.*, 2022). It has been shown that poor circulation of nitrogen and phosphorus during AD inhibits the metabolic activity of microorganisms and ultimately affects the stability of the system operation.

In summary, when the  $\text{NH}_4^+\text{-N}$  concentration increased to 4214.5 mg/L, the ammonia inhibition effect in the system was significantly intensified, and the damage to methanogens had become irreversible. This concentration substantially exceeded the conventional  $\text{NH}_4^+\text{-N}$  tolerance threshold for AD (typically <3000 mg/L), indicating that the  $\text{NH}_4^+\text{-N}$  accumulation risk associated with CM substrates warrants particular attention.

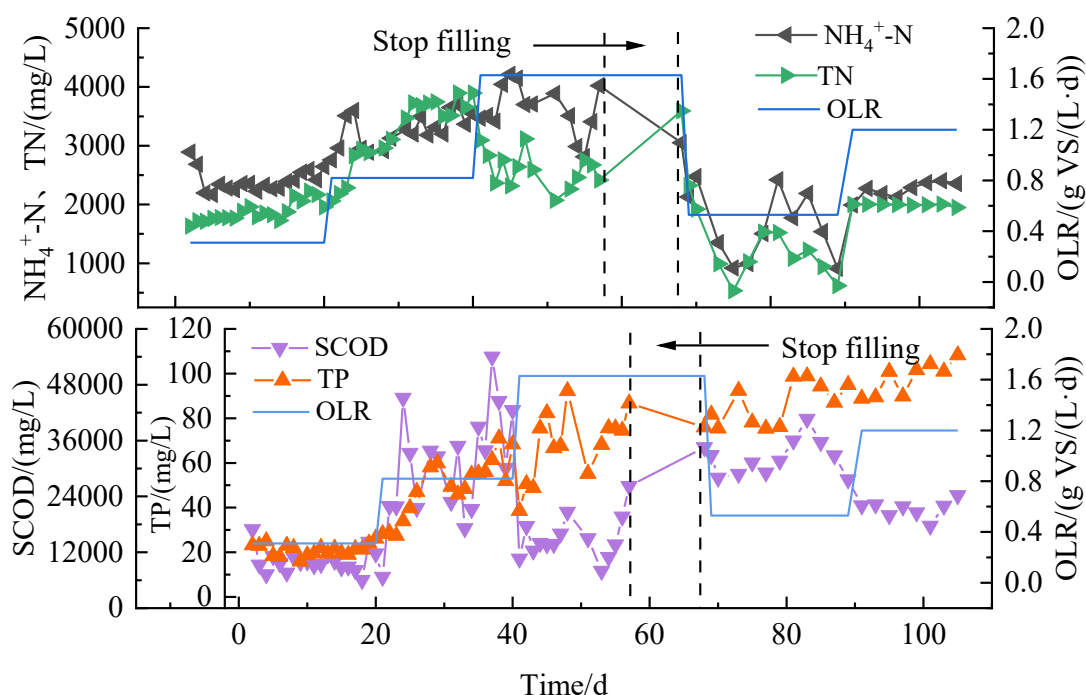


Fig. 5 - Concentrations of  $\text{NH}_4^+\text{-N}$ , TN, SCOD, and TP in digestate effluent

#### Analysis of nutrient changes in digestate effluent

After AD of CM, 90% of the nutrients are retained in the digestate except for a large loss of carbon, especially nitrogen, phosphorus, and potassium, which are large and can be directly absorbed by crops. Therefore, digestate can be considered an efficient and high-quality liquid organic fertilizer. Fig. 6 shows the results of nutrient composition of digestate effluent at different stages of digestion, from which it can be seen that pH fluctuated slightly with OLR, but generally remained within the range suitable for AD (7.6-8.4), and the content of OM, HN, AK, and AP did not vary much in the digestate effluent produced at different OLR. At an OLR of 0.53 g VS/(L·d), the content of each nutrient was relatively high. The contents of OM, HN, AK, and AP in the digestate effluent were 15.23 ( $\pm 0.71$ ) g/kg, 1,896.67 ( $\pm 215.95$ ) mg/kg, 14.73 ( $\pm 0.47$ ) mg/kg, and 3,970 ( $\pm 242.69$ ) mg/kg, respectively. This phenomenon is primarily attributed to the impaired metabolic function of the system, where the hydrolysis-acidification process dominated while the methanogenesis stage was inhibited, resulting in the accumulation of nitrogen, phosphorus, potassium, and other nutrients in the liquid phase. Therefore, the elevated nutrient concentration under this condition does not indicate an improvement in AD performance, but rather reflects that the reaction system was in a metastable state with incomplete substrate degradation. According to the "Greening Planting Soil" (CJ/T 340-2016) the technical requirements are (20~80) g/kg, (40~200) mg/kg, (5~60) mg/kg, and (60~300) mg/kg, respectively. These results indicate that the nutrient content of the digestate effluent significantly exceeds the standard limits. Therefore, when used as a fertilizer, the digestate should be applied only after appropriate treatment or dilution and mixing with soil.

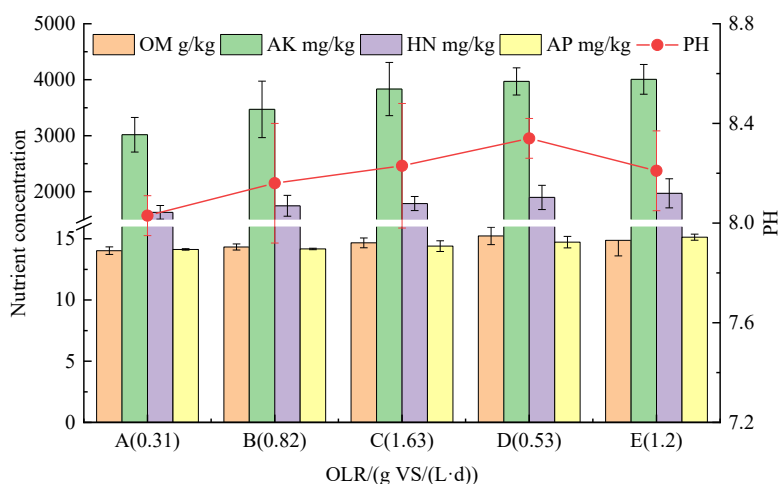


Fig. 6 - Concentration of nutrients in digestate effluent

### Changes in the diversity of bacterial communities

To study the changes in the relative abundance of dominant bacterial communities under different OLR, a total of 15 samples were obtained by sampling three times at different times under the same OLR. High-throughput sequencing was performed on the 15 samples to obtain the relative abundance maps of bacterial and archaeal communities. The sampling arrangement is shown in Table 5.

Fig. 7 shows the relative abundance of bacterial communities. Fig. 7(a) shows the relative abundance changes at the level of bacterial phylum, from which it can be seen that *Firmicutes*, *Bacteroidota*, and *Proteobacteria* were the dominant phyla throughout the AD process, and all of these bacteria have the ability to hydrolyse and acidify the more complex OM (e.g., proteins and carbohydrates).

*Firmicutes* remained absolutely dominant throughout the reaction. *Bacteroidota* and *proteobacteria*, as subdominant phyla, showed different trends. At an OLR of 0.31 g VS/(L·d), *Firmicutes* dominated the bacterial community with a relative abundance higher than 40%, followed by *Bacteroidota* (higher than 22%) and *Proteobacteria* (higher than 5%).

*Firmicutes* abundance remained highest when the OLR was 0.82-1.63 g VS/(L·d). This may be because *Firmicute* phylum bacteria are highly environmentally adapted in that they are able to form endospores to defend themselves against undesirable environments, such as heavily acidified environments, which allows them to maintain high relative abundance during AD even under highly variable conditions (Galperin *et al.*, 2016). For example, in one study, the relative abundance of *Firmicutes* in AD reactors was maintained at 62% to 95%, even under high OLR conditions (Fykse *et al.*, 2016). The relative abundance of *Bacteroidota* and *Proteobacteria* began to decrease under this OLR, probably because the rate of VFAs production in the AD system was greater than the rate of their utilisation by methanogens under high OLR, leading to the accumulation of VFAs, which cause toxicity to the microbial cells, affecting their normal metabolism and growth, and thus inhibiting the growth of *Bacteroidota* and *Proteobacteria* (Cao *et al.*, 2025). When the OLR was readjusted to 0.53 and 1.20 g VS/(L·d), the abundance of *Firmicutes* decreased to the level observed at 0.31 g VS/(L·d), indicating that its optimal OLR range was 0.82-1.63 g VS/(L·d). Within this range, the abundance of both *Bacteroidetes* and *Proteobacteria* showed an increasing trend, which may be attributed to the alleviation of acidification stress and the subsequent recovery of metabolic activity in *Bacteroidetes*. *Synergistota* can generate acetate, hydrogen, and carbon dioxide through the degradation of glucose, organic acids, etc., which are important intermediary products in the AD process. *Synergistota* only appeared at an OLR of 0.31 g VS/(L·d), which may be because microorganisms in the *Synergistota* phylum may be more sensitive to environmental changes, and their growth and reproduction were inhibited under high OLR due to drastic changes in environmental conditions (Yellezuome *et al.*, 2024).

Fig. 7(b) shows the relative abundance changes at the level of bacterial genus, at OLR of 0.31 gVS/(L·d). The abundance of the *Mobilitalea* genus showed a decreasing trend as the reaction proceeded, and subsequently remained stable in the following reaction stages. The *Mobilitalea* genus belongs to the *Firmicutes*, and its polysaccharide-degrading and acid-producing functions are able to accelerate the initiation and conduct of anaerobic fermentation and shorten the fermentation cycle. By promoting the production of VFAs and methane, the *Mobilitalea* genus can help to improve the quality of biogas and increase the methane content in biogas.

From the 21st day to the end of the reaction, more OM was decomposed, which promoted the growth and reproduction of the *Bacteroides* genus, making the *Bacteroides* genus become a dominant bacterium. The *Bacteroides* genus was able to utilise polysaccharides as a carbon source, as well as proteins and amino acids as a source of nitrogen and energy, which promoted its growth and reproduction. Under high OLR, the relative abundance of the *Bacteroides* genus increased and became one of the dominant genera, indicating that they are more competitive under a high OLR environment. At relatively low OLR, the relative abundance of the *Breznakibacter* genus was higher, which can secrete hydrolytic enzymes such as cellulase and xylanase to hydrolyse complex cellulose and lignocellulose into small molecules of sugars. Its ability to break down cellulose-like substances in CM plays an important role in promoting the hydrolysis of anaerobically digested substrates. The relative abundance of the *Breznakibacter* genus began to decrease under high OLR, probably due to the changes in environmental conditions, which were unfavourable to the growth and metabolism of the *Breznakibacter* genus and thus led to the decrease in its abundance. *Fermentimonas* belongs to the phylum *Bacteroidetes*, a hydrogenotrophic methanotrophic bacterium that exhibited relatively high abundance only at an OLR of 0.31 g VS/(L·d). It has been shown that *Fermentimonas* is able to increase the production of H<sub>2</sub>, which in turn facilitates the generation of CH<sub>4</sub> through H<sub>2</sub> reduction of CO<sub>2</sub> (Wang *et al.*, 2023). Combined with the daily methane production in Fig. 4 (b), this suggests that *Fermentimonas* has a promoting effect on AD for methane production.

Table 5

Sampling arrangement for microbial testing					
OLR [g VS/(L·d)]	0.31	0.82	1.63	0.53	1.20
Sampling time [d]	5, 7, 14	21, 28, 38	44, 48, 55	69, 75, 83	93, 99, 103

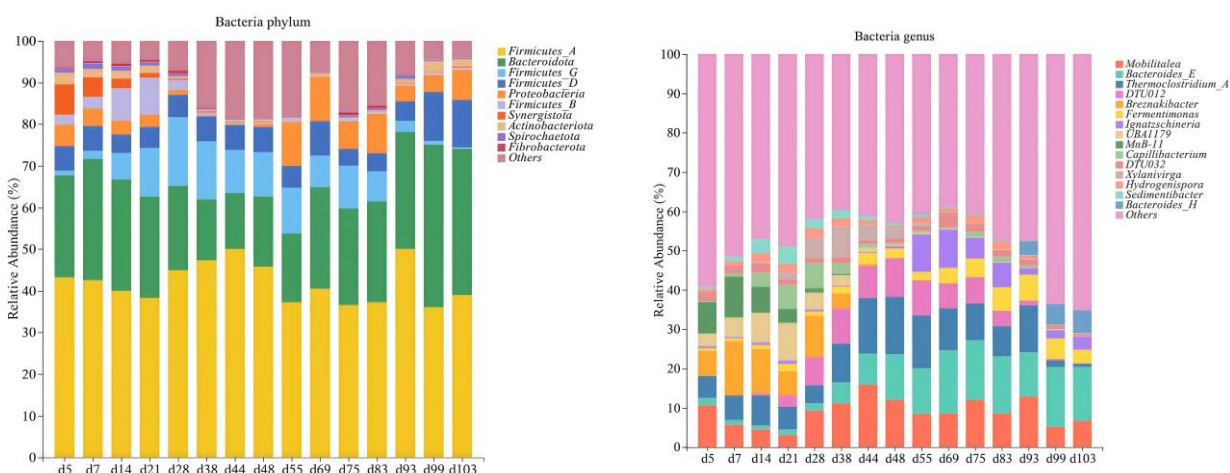


Fig. 7 - Relative abundance of bacterial communities

(a) Relative abundance of the first 10 phyla

(b) Relative abundance of the top 15 genera

### Changes in the diversity of archaeal communities

Fig. 8 shows the changes in relative abundance of archaeal communities at the phylum and genus level. From Fig. 8(a), it can be seen that the dominant bacterial group at all stages of the experiment was *Halobacteriota*. *Halobacteriota* contained most of the groups in Archaea, such as *Archaeoglobi*, *Halobacteria*, and *Methanomicrobia*. When the OLR was 0.53 g VS/(L·d), the relative abundance of *Thermoplasmatota* was higher. As can be seen in Fig. 8(b), the dominant bacterium at the genus level was *Methanosarcina* in the pre-intermediate stage. It is a methanogenic archaeon that decomposes acetic acid and then oxidises the carboxyl group to CO<sub>2</sub>, reduces the methyl group to methane, and has a good tolerance to high NH<sub>4</sub><sup>+</sup>-N environments. After the reaction had destabilised on day 58, the abundance of *Methanosarcina* decreased rapidly. The relative abundance of *Methanoculleus* increased when the OLR decreased from 1.63 g VS/(L·d) to 0.53 g VS/(L·d). The relative abundance of *Methanocorpusculum* increased when the OLR was 1.20 g VS/(L·d). It was shown that both *Methanoculleus* and *Methanocorpusculum* could not utilise acetic acid and methylamine (Zhang *et al.*, 2022), resulting in a decrease in gas production performance in the later stages of the reaction and a gradual decrease in methane yield.

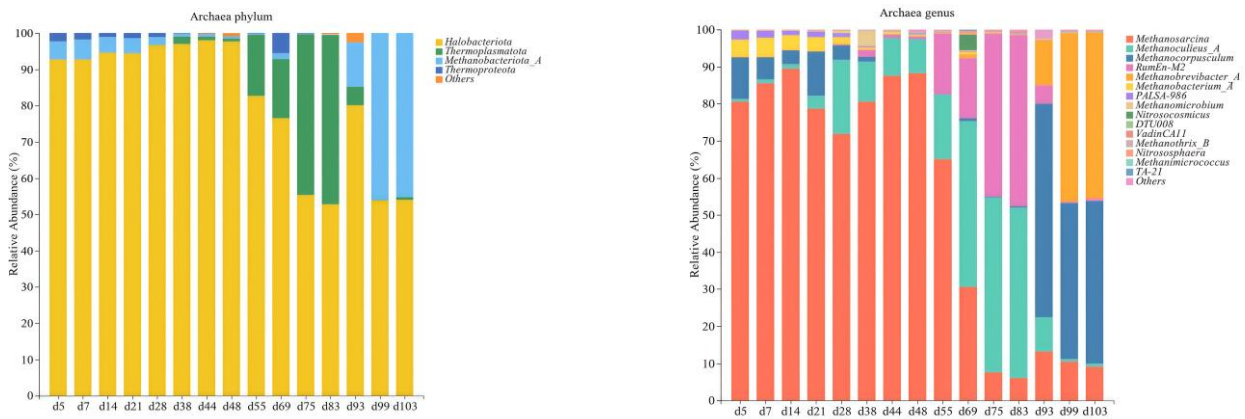


**Fig. 8 - Relative abundance of archaeal communities**  
 (a) Relative abundance of the first 10 phyla (b) Relative abundance of the first 15 genera

**Correlation analysis between the abundance of bacterial flora and various physicochemical indicators**

In order to analyse the correlation between each physicochemical index and the abundance of bacteria during AD, the top 20 genera of relative abundance were selected to draw heat maps. Fig. 9 shows the Spearman correlation between the relative abundance of bacteria and archaea and each physicochemical index. As can be seen from the figure, *Sedimentibacter*, *Breznakibacter*, *Methanosarcina*, and *Methanobacterium* showed significant positive correlation with methane production and significant negative correlation with AP. *Bacteroides* and *Fermentimonas* showed a significant positive correlation with AP and a significant negative correlation with methane production. *Methanosarcina* showed a positive correlation with  $NH_4^+-N$ . Some of the unnamed microbial communities showed significant correlations with the physicochemical indicators, which still need to be investigated. *DTU012* and *Xylanivirga* showed significant positive correlations with AK and  $NH_4^+-N$ . *Methanimicrococcus* and *Methanoculleus* showed positive correlations with AP and AK, respectively. OM and HN were not significantly correlated with the microbial communities of the top 20 genera.

The above analysis showed that *Sedimentibacter*, *Breznakibacter*, *Methanosarcina*, and *Methanobacterium* had a significant effect on increasing the efficiency of gas production, and *Bacteroides* and *Fermentimonas* had a significant effect on increasing the concentration of AP in the digestate effluent. The microbial communities affecting HN, AK, and OM in the digestate effluent are not clear. During AD, it is not easy to achieve higher levels of nutrient content in the digestate effluent while increasing the gas production efficiency, since the association of gas production efficiency and nutrient content with the same microorganisms shows an inverse relationship.

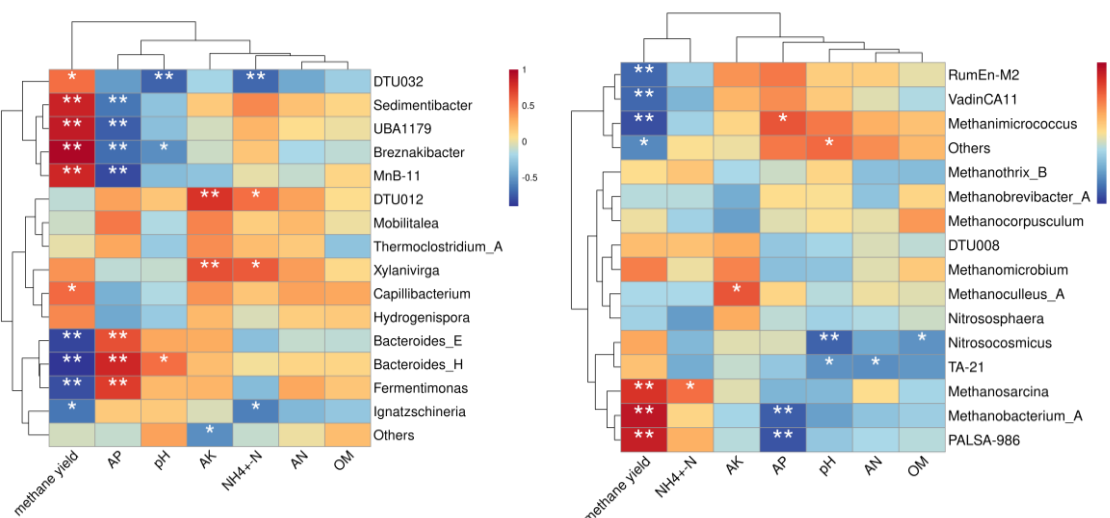


**Fig. 9 - Spearman's correlation between physical and chemical indicators and relative abundance of microorganisms (Note: \* indicates  $p < 0.05$ , \*\* indicates  $p < 0.01$ )**  
 (a) Correlation with bacterial genera (b) Correlation with the genus Archaea

## CONCLUSIONS

This study systematically investigated the ACoD characteristics of CM and CS through batch and semi-continuous experiments. The main conclusions are as follows: (1) Optimal OLR and ammonia inhibition threshold. The semi-continuous flow system achieved the highest methane yield at an OLR of 0.31 g VS/(L·d); however, when the OLR increased to 1.63 g VS/(L·d),  $\text{NH}_4\text{-N}$  concentration accumulated to 4214.5 mg/L, exceeding the tolerance limit of methanogens and resulting in irreversible damage, even though lowering the OLR could not restore the system. (2) "High biogas production-weak synergy" characteristics. Batch experiments indicated that although the CM+CS combination exhibited the optimal methane yield (82.45 mL/g VS), its synergistic enhancement effect was weaker than that of SM and DM systems, suggesting that biogas production performance is governed by multiple factors including C/N ratio compatibility and buffering capacity. (3) Identification of key functional microorganisms. *Firmicutes*, *Bacteroidota*, and *Proteobacteria* were identified as the dominant phyla; *Sedimentibacter*, *Breznakibacter*, *Methanosarcina*, and *Methanobacterium* showed significant positive correlations with methane yield, while *Fermentimonas* could promote the methanogenesis process. This study clarified the optimal operating parameters, critical ammonia inhibition threshold, and microbial regulation mechanisms for ACoD of CM and CS, providing theoretical basis and technical reference for the engineering application of high  $\text{NH}_4\text{-N}$  feedstocks.

In summary, this study elucidated the characteristics of ACoD of CM and CS, with particular emphasis on revealing the dynamic patterns of anaerobic microbial community abundance, thereby providing a theoretical foundation for enhancing methane yield through artificial manipulation of dominant microflora. However, this study relied primarily on high-throughput sequencing technology, focusing on the characterization of microbial community structure and abundance dynamics, without in-depth resolution of functional gene expression levels and metabolic pathway activities. Therefore, future research will incorporate multi-omics approaches, including metagenomics, metatranscriptomics, and metaproteomics, to systematically elucidate the metabolic mechanisms of anaerobic microorganisms at the levels of gene function, transcriptional activity, and protein expression. This comprehensive characterization of microbial functional traits during the co-digestion process aims to provide deeper scientific insights for optimizing AD performance.

## ACKNOWLEDGEMENT

This study was financially supported by the annual innovation research plan of Daqing Petroleum Management Bureau Co., Ltd. (Daqing, China) (No. dqc-2021-qt-ky-001), Heilongjiang Bayi Agricultural University Natural Science Talent Support Plan (No. ZRCQC202005), Heilongjiang Bayi Agricultural University Talent Research Initiation Plan (No. XYB202001) and Heilongjiang Bayi Agricultural University Natural Science Talent Support Program (No. ZRCPY202206).

## REFERENCES

- [1] Cao, Q., Meng, X., Jia, F., Li, J., Liu, X., & Li, D. (2025). The metabolic redundancy relieving VFAs shocks in anaerobic digestion system exposed sequentially to increasing acetic acid loading. *Chemical Engineering Journal*, vol. 505, pp.159791.
- [2] Duan, H., He, P., Zhang, H., Shao, L., & Lü, F. (2022). Metabolic regulation of mesophilic *Methanosarcina barkeri* to ammonium inhibition. *Environmental Science & Technology*, vol.56, no.12, pp.8897-8907.
- [3] Duan Ngo, T., Khudur, L. S., Hassan, S., Jansrihibul, K., & Ball, A. S. (2024). Enhancing microbial viability with biochar for increased methane production during the anaerobic digestion of chicken manure. *Fuel*, vol.368, pp.131603.
- [4] Fykse, E. M., Aarskaug, T., Madslien, E. H., & Dybwad, M. (2016). Microbial community structure in a full-scale anaerobic treatment plant during start-up and first year of operation revealed by high-throughput 16S rRNA gene amplicon sequencing. *Bioresource Technology*, vol. 222, pp. 380-387.
- [5] Galperin, M. Y. (2016). Genome diversity of spore-forming Firmicutes. *The bacterial spore: From molecules to systems*, pp.1-18.
- [6] Guo, H. G., Li, Q., Wang, L. L., Chen, Q. L., Hu, H. W., Cheng, D. J., & He, J. Z. (2022). Semi-solid state promotes the methane production during anaerobic co-digestion of chicken manure with corn straw comparison to wet and high-solid state. *Journal of Environmental Management*, vol.316, pp.115264.

- [7] Gong, S.Y., (2020). *Study on the maximum organic loading capacity of anaerobic fermentation with solar temperature control* (太阳能控温的厌氧发酵最大有机负荷处理能力研究), MSc Thesis, Lanzhou University of Technology, Lanzhou, China.
- [8] He, H., Zhang, Z., Ma, S., Khan, M. U., Peng, Z., Geng, H., ... & Yuan, X. (2025). Mitigation of ammonia inhibition in dry anaerobic digestion of chicken manure and corn straw using a self-developed gradient anaerobic digestion reactor. *Energy*, vol.332, pp.137256.
- [9] Khatun, M. L., Nime, J., Alam, M. M., & Saha, C. K. (2025). Co-digestion of poultry droppings with maize cob for bioenergy and bio-fertilizer production. *Fuel*, vol.386, pp.134270.
- [10] Koul, B., Yakoob, M., & Shah, M. P. (2022). Agricultural waste management strategies for environmental sustainability. *Environmental Research*, vol. 206, pp.112285.
- [11] Karki, R., Chuenchart, W., Surendra, K. C., Shrestha, S., Raskin, L., Sung, S., ... & Khanal, S. K. (2021). Anaerobic co-digestion: Current status and perspectives. *Bioresource Technology*, vol. 330, pp.125001.
- [12] Mlinar, S., Weig, A. R., & Freitag, R. (2022). Influence of NH<sub>3</sub> and NH<sub>4</sub><sup>+</sup> on anaerobic digestion and microbial population structure at increasing total ammonia nitrogen concentrations. *Bioresource technology*, vol.361, pp.127638.
- [13] Song, Y., Qiao, W., Zhang, J., & Dong, R. (2023). Process performance and functional microbial community in the anaerobic digestion of chicken manure: a review. *Energies*, vol. 16, no.12, pp.4675.
- [14] Sun, G.D., Ma, J.Y., Hao, S., Dong, H., Zhao, X.R., Chai, Q.L. & Dang, Y., (2025), Research progress on key influencing factors of methane production efficiency from livestock and poultry manure anaerobic digestion (畜禽粪污厌氧消化产甲烷效能的关键影响因素研究进展), *Environmental Engineering*, vol.43, no.3, pp.114-129.
- [15] Wang, M., Wu, C., & Li, C. (2024). Anaerobic Co-Digestion of Chicken Manure and Corn Straw: Gas Production, Biogas Fertilizer Effectiveness, and Microbial Diversity. *Water, Air, & Soil Pollution*, vol.235, no.6, pp.365.
- [16] Wang, N., Yang, Y., Xu, K., Long, X., Liu, H., Zhang, Y., ... & Li, J. (2023). Insight into the metabolic pathway of EAD based on metabolic flux, microbial community, and enzyme activity. *Biochemical Engineering Journal*, vol.196, pp.108938.
- [17] Xu, H., Guo, L., Gao, M., Zhao, Y., Jin, C., Ji, J., & She, Z. (2022). Comparison on anaerobic phosphorus release and recovery from waste activated sludge by different chemical pretreatment methods: Focus on struvite quality and benefit analysis. *Science of The Total Environment*, vol.825, pp.154110.
- [18] Yellezuome, D., Zhu, X., Liu, X., Liu, R., Sun, C., Abd-Alla, M. H., & Rasmey, A. H. M. (2024). Effects of organic loading rate on hydrogen and methane production in a novel two-stage reactor system: performance, enzyme activity and microbial structure. *Chemical Engineering Journal*, vol.480, pp.148055.
- [19] Zhan, Y., Cao, X., & Zhu, J. (2026). Enhanced bioenergy production via operational optimization of anaerobic co-digestion of chicken litter and straw waste with magnetite nanoparticles. *Energy*, vol.347, pp.140428.
- [20] Zheng, S., Yang, F., Huang, W., Lei, Z., Zhang, Z., & Huang, W. (2022). Combined effect of zero valent iron and magnetite on semi-dry anaerobic digestion of swine manure. *Bioresource Technology*, vol.346, pp.126438
- [21] Zhang, H., Yuan, W., Dong, Q., Wu, D., Yang, P., Peng, Y., ... & Peng, X. (2022). Integrated multi-omics analyses reveal the key microbial phylotypes affecting anaerobic digestion performance under ammonia stress. *Water research*, vol.213, pp.118152.
- [22] Zhu, X., Yellezuome, D., Liu, R., Wang, Z., & Liu, X. (2022). Effects of co-digestion of food waste, corn straw and chicken manure in two-stage anaerobic digestion on trace element bioavailability and microbial community composition. *Bioresource technology*, vol.346, pp.126625.
- [23] Zhang, L., Tian, H., Lee, J. T., Lim, J. W., Loh, K. C., Dai, Y., & Tong, Y. W. (2022). Bioaugmentation strategies via acclimatized microbial consortia for bioenergy production. *Biomass, Biofuels, Biochemicals*, pp. 179-214.
- [24] Zhu, X., Yellezuome, D., Liu, R., Wang, Z., & Liu, X. (2022). Effects of co-digestion of food waste, corn straw and chicken manure in two-stage anaerobic digestion on trace element bioavailability and microbial community composition. *Bioresource technology*, vol.346, pp.126625.